# Measurement of the Ratio of $B^+$ and $B^0$ Meson Lifetimes

V. M. Abazov,[33] B. Abbott,[70] M. Abolins,[61] B. S. Acharya,[27] M. Adams,[48] T. Adams,[46] M. Agelou,[17] J.-L. Agram,[18] S. H. Ahn,[29] M. Ahsan,[55] G. D. Alexeev,[33] G. Alkhazov,[37] A. Alton,[60] G. Alverson,[59] G. A. Alves,[2] M. Anastasoaie,[32] S. Anderson,[42] B. Andrieu,[16] Y. Arnoud,[13] A. Askew,[74] B. Åsman,[38] O. Atramentov,[53] C. Autermann,[20] C. Avila,[7] F. Badaud,[12] A. Baden,[57] B. Baldin,[47] P. W. Balm,[31] S. Banerjee,[27] E. Barberis,[59] P. Bargassa,[74] P. Baringer,[54] C. Barnes,[40] J. Barreto,[2] J. F. Bartlett,[47] U. Bassler,[16] D. Bauer,[51] A. Bean,[54] S. Beauceron,[16] M. Begel,[66] A. Bellavance,[63] S. B. Beri,[26] G. Bernardi,[16] R. Bernhard,[47,*] I. Bertram,[39] M. Besançon,[17] R. Beuselinck,[40] V. A. Bezzubov,[36] P. C. Bhat,[47] V. Bhatnagar,[26] M. Binder,[24] K. M. Black,[58] I. Blackler,[40] G. Blazey,[49] F. Blekman,[31] S. Blessing,[46] D. Bloch,[18] U. Blumenschein,[22] A. Boehnlein,[47] O. Boeriu,[52] T. A. Bolton,[55] F. Borcherding,[47] G. Borissov,[39] K. Bos,[31] T. Bose,[65] A. Brandt,[72] R. Brock,[61] G. Brooijmans,[65] A. Bross,[47] N. J. Buchanan,[46] D. Buchholz,[50] M. Buehler,[48] V. Buescher,[22] S. Burdin,[47] T. H. Burnett,[76] E. Busato,[16] J. M. Butler,[58] J. Bystricky,[17] W. Carvalho,[3] B. C. K. Casey,[71] N. M. Cason,[52] H. Castilla-Valdez,[30] S. Chakrabarti,[27] D. Chakraborty,[49] K. M. Chan,[66] A. Chandra,[27] D. Chapin,[71] F. Charles,[18] E. Cheu,[42] L. Chevalier,[17] D. K. Cho,[66] S. Choi,[45] T. Christiansen,[24] L. Christofek,[54] D. Claes,[63] B. Clément,[18] C. Clément,[38] Y. Coadou,[5] M. Cooke,[74] W. E. Cooper,[47] D. Coppage,[54] M. Corcoran,[74] J. Coss,[19] A. Cothenet,[14] M.-C. Cousinou,[14] S. Crépé-Renaudin,[13] M. Cristetiu,[45] M. A. C. Cummings,[49] D. Cutts,[71] H. da Motta,[2] B. Davies,[39] G. Davies,[40] G. A. Davis,[50] K. De,[72] P. de Jong,[31] S. J. de Jong,[32] E. De La Cruz-Burelo,[30] C. De Oliveira Martins,[3] S. Dean,[41] F. Déliot,[17] P. A. Delsart,[19] M. Demarteau,[47] R. Demina,[66] P. Demine,[17] D. Denisov,[47] S. P. Denisov,[36] S. Desai,[67] H. T. Diehl,[47] M. Diesburg,[47] M. Doidge,[39] H. Dong,[67] S. Doulas,[59] L. Duflot,[15] S. R. Dugad,[27] A. Duperrin,[14] J. Dyer,[61] A. Dyshkant,[49] M. Eads,[49] D. Edmunds,[61] T. Edwards,[41] J. Ellison,[45] J. Elmsheuser,[24] J. T. Eltzroth,[72] V. D. Elvira,[47] S. Eno,[57] P. Ermolov,[35] O. V. Eroshin,[36] J. Estrada,[47] D. Evans,[40] H. Evans,[65] A. Evdokimov,[34] V. N. Evdokimov,[36] J. Fast,[47] S. N. Fatakia,[58] L. Feligioni,[58] T. Ferbel,[66] F. Fiedler,[24] F. Filthaut,[32] W. Fisher,[64] H. E. Fisk,[47] M. Fortner,[49] H. Fox,[22] W. Freeman,[47] S. Fu,[47] S. Fuess,[47] T. Gadfort,[76] C. F. Galea,[32] E. Gallas,[47] E. Galyaev,[52] C. Garcia,[66] A. Garcia-Bellido,[76] J. Gardner,[54] V. Gavrilov,[34] P. Gay,[12] D. Gelé,[18] R. Gelhaus,[45] K. Genser,[47] C. E. Gerber,[48] Y. Gershtein,[71] G. Ginther,[66] T. Golling,[21] B. Gómez,[7] K. Gounder,[47] A. Goussiou,[52] P. D. Grannis,[67] S. Greder,[18] H. Greenlee,[47] Z. D. Greenwood,[56] E. M. Gregores,[4] Ph. Gris,[12] J.-F. Grivaz,[15] L. Groer,[65] S. Grünendahl,[47] M. W. Grünewald,[28] S. N. Gurzhiev,[36] G. Gutierrez,[47] P. Gutierrez,[70] A. Haas,[65] N. J. Hadley,[57] S. Hagopian,[46] I. Hall,[70] R. E. Hall,[44] C. Han,[60] L. Han,[41] K. Hanagaki,[47] K. Harder,[55] R. Harrington,[59] J. M. Hauptman,[53] R. Hauser,[61] J. Hays,[50] T. Hebbeker,[20] D. Hedin,[49] J. M. Heinmiller,[48] A. P. Heinson,[45] U. Heintz,[58] C. Hensel,[54] G. Hesketh,[59] M. D. Hildreth,[52] R. Hirosky,[75] J. D. Hobbs,[67] B. Hoeneisen,[11] M. Hohlfeld,[23] S. J. Hong,[29] R. Hooper,[71] P. Houben,[31] Y. Hu,[67] J. Huang,[51] I. Iashvili,[45] R. Illingworth,[47] A. S. Ito,[47] S. Jabeen,[54] M. Jaffré,[15] S. Jain,[70] V. Jain,[68] K. Jakobs,[22] A. Jenkins,[40] R. Jesik,[40] K. Johns,[42] M. Johnson,[47] A. Jonckheere,[47] P. Jonsson,[40] H. Jöstlein,[47] A. Juste,[47] M. M. Kado,[43] D. Käfer,[20] W. Kahl,[55] S. Kahn,[68] E. Kajfasz,[14] A. M. Kalinin,[33] J. Kalk,[61] D. Karmanov,[35] J. Kasper,[58] D. Kau,[46] R. Kehoe,[73] S. Kermiche,[14] S. Kesisoglou,[71] A. Khanov,[66] A. Kharchilava,[52] Y. M. Kharzheev,[33] K. H. Kim,[29] B. Klima,[47] M. Klute,[21] J. M. Kohli,[26] M. Kopal,[70] V. M. Korablev,[36] J. Kotcher,[68] B. Kothari,[65] A. Koubarovsky,[35] A. V. Kozelov,[36] J. Kozminski,[61] S. Krzywdzinski,[47] S. Kuleshov,[34] Y. Kulik,[47] S. Kunori,[57] A. Kupco,[17] T. Kurča,[19] S. Lager,[38] N. Lahrichi,[17] G. Landsberg,[71] J. Lazoflores,[46] A.-C. Le Bihan,[18] P. Lebrun,[19] S. W. Lee,[29] W. M. Lee,[46] A. Leflat,[35] F. Lehner,[47,*] C. Leonidopoulos,[65] P. Lewis,[40] J. Li,[72] Q. Z. Li,[47] J. G. R. Lima,[49] D. Lincoln,[47] S. L. Linn,[46] J. Linnemann,[61] V. V. Lipaev,[36] R. Lipton,[47] L. Lobo,[40] A. Lobodenko,[37] M. Lokajicek,[10] A. Lounis,[18] H. J. Lubatti,[76] L. Lueking,[47] M. Lynker,[52] A. L. Lyon,[47] A. K. A. Maciel,[49] R. J. Madaras,[43] P. Mättig,[25] A. Magerkurth,[60] A.-M. Magnan,[13] N. Makovec,[15] P. K. Mal,[27] S. Malik,[56] V. L. Malyshev,[33] H. S. Mao,[6] Y. Maravin,[47] M. Martens,[47] S. E. K. Mattingly,[71] A. A. Mayorov,[36] R. McCarthy,[67] R. McCroskey,[42] D. Meder,[23] H. L. Melanson,[47] A. Melnitchouk,[62] M. Merkin,[35] K. W. Merritt,[47] A. Meyer,[20] H. Miettinen,[74] D. Mihalcea,[49] J. Mitrevski,[65] N. Mokhov,[47] J. Molina,[3] N. K. Mondal,[27] H. E. Montgomery,[47] R. W. Moore,[5] G. S. Muanza,[19] M. Mulders,[47] Y. D. Mutaf,[67] E. Nagy,[14] M. Narain,[58] N. A. Naumann,[32] H. A. Neal,[60] J. P. Negret,[7] S. Nelson,[46] P. Neustroev,[37] C. Noeding,[22] A. Nomerotski,[47] S. F. Novaes,[4] T. Nunnemann,[24] E. Nurse,[41] V. O'Dell,[47] D. C. O'Neil,[5] V. Oguri,[3] N. Oliveira,[3] N. Oshima,[47] G. J. Otero y Garzón,[48] P. Padley,[74] N. Parashar,[56] J. Park,[29] S. K. Park,[29] J. Parsons,[65] R. Partridge,[71] N. Parua,[67] A. Patwa,[68] P. M. Perea,[45] E. Perez,[17] O. Peters,[31] P. Pétroff,[15] M. Petteni,[40] L. Phaf,[31] R. Piegaia,[1] P. L. M. Podesta-Lerma,[30] V. M. Podstavkov,[47] Y. Pogorelov,[52] B. G. Pope,[61] W. L. Prado da Silva,[3] H. B. Prosper,[46] S. Protopopescu,[68] M. B. Przybycien,[50,†] J. Qian,[60] A. Quadt,[21] B. Quinn,[62] K. J. Rani,[27] P. A. Rapidis,[47] P. N. Ratoff,[39] N. W. Reay,[55] S. Reucroft,[59] M. Rijssenbeek,[67]

 © 2005 The American Physical Society

I. Ripp-Baudot,[18] F. Rizatdinova,[55] C. Royon,[17] P. Rubinov,[47] R. Ruchti,[52] G. Sajot,[13] A. Sánchez-Hernández,[30] M. P. Sanders,[41] A. Santoro,[3] G. Savage,[47] L. Sawyer,[56] T. Scanlon,[40] R. D. Schamberger,[67] H. Schellman,[50] P. Schieferdecker,[24] C. Schmitt,[25] A. A. Schukin,[36] A. Schwartzman,[64] R. Schwienhorst,[61] S. Sengupta,[46] H. Severini,[70] E. Shabalina,[48] M. Shamim,[55] V. Shary,[17] W. D. Shephard,[52] D. Shpakov,[59] R. A. Sidwell,[55] V. Simak,[9] V. Sirotenko,[47] P. Skubic,[70] P. Slattery,[66] R. P. Smith,[47] K. Smolek,[9] G. R. Snow,[63] J. Snow,[69] S. Snyder,[68] S. Söldner-Rembold,[41] X. Song,[49] Y. Song,[72] L. Sonnenschein,[58] A. Sopczak,[39] M. Sosebee,[72] K. Soustruznik,[8] M. Souza,[2] B. Spurlock,[72] N. R. Stanton,[55] J. Stark,[13] J. Steele,[56] G. Steinbrück,[65] K. Stevenson,[51] V. Stolin,[34] A. Stone,[48] D. A. Stoyanova,[36] J. Strandberg,[38] M. A. Strang,[72] M. Strauss,[70] R. Ströhmer,[24] M. Strovink,[43] L. Stutte,[47] S. Sumowidagdo,[46] A. Sznajder,[3] M. Talby,[14] P. Tamburello,[42] W. Taylor,[5] P. Telford,[41] J. Temple,[42] S. Tentindo-Repond,[46] E. Thomas,[14] B. Thooris,[17] M. Tomoto,[47] T. Toole,[57] J. Torborg,[52] S. Towers,[67] T. Trefzger,[23] S. Trincaz-Duvoid,[16] B. Tuchming,[17] C. Tully,[64] A. S. Turcot,[68] P. M. Tuts,[65] L. Uvarov,[37] S. Uvarov,[37] S. Uzunyan,[49] B. Vachon,[5] R. Van Kooten,[51] W. M. van Leeuwen,[31] N. Varelas,[48] E. W. Varnes,[42] I. A. Vasilyev,[36] M. Vaupel,[25] P. Verdier,[15] L. S. Vertogradov,[33] M. Verzocchi,[57] F. Villeneuve-Seguier,[40] J.-R. Vlimant,[16] E. Von Toerne,[55] M. Vreeswijk,[31] T. Vu Anh,[15] H. D. Wahl,[46] R. Walker,[40] L. Wang,[57] Z.-M. Wang,[67] J. Warchol,[52] M. Warsinsky,[21] G. Watts,[76] M. Wayne,[52] M. Weber,[47] H. Weerts,[61] M. Wegner,[20] N. Wermes,[21] A. White,[72] V. White,[47] D. Whiteson,[43] D. Wicke,[47] D. A. Wijngaarden,[32] G. W. Wilson,[54] S. J. Wimpenny,[45] J. Wittlin,[58] M. Wobisch,[47] J. Womersley,[47] D. R. Wood,[59] T. R. Wyatt,[41] Q. Xu,[60] N. Xuan,[52] R. Yamada,[47] M. Yan,[57] T. Yasuda,[47] Y. A. Yatsunenko,[33] Y. Yen,[25] K. Yip,[68] S. W. Youn,[50] J. Yu,[72] A. Yurkewicz,[61] A. Zabi,[15] A. Zatserklyaniy,[49] M. Zdrazil,[67] C. Zeitnitz,[23] D. Zhang,[47] X. Zhang,[70] T. Zhao,[76] Z. Zhao,[60] B. Zhou,[60] J. Zhu,[57] M. Zielinski,[66] D. Zieminska,[51] A. Zieminski,[51] R. Zitoun,[67] V. Zutshi,[49] E. G. Zverev,[35] and A. Zylberstejn[17]

(D0 Collaboration)

[1]*Universidad de Buenos Aires, Buenos Aires, Argentina*
[2]*LAFEX, Centro Brasileiro de Pesquisas Físicas, Rio de Janeiro, Brazil*
[3]*Universidade do Estado do Rio de Janeiro, Rio de Janeiro, Brazil*
[4]*Instituto de Física Teórica, Universidade Estadual Paulista, São Paulo, Brazil*
[5]*Simon Fraser University, Burnaby, Canada; University of Alberta, Edmonton, Canada, McGill University, Montreal, Canada; and York University, Toronto, Canada*
[6]*Institute of High Energy Physics, Beijing, People's Republic of China*
[7]*Universidad de los Andes, Bogotá, Colombia*
[8]*Charles University, Center for Particle Physics, Prague, Czech Republic*
[9]*Czech Technical University, Prague, Czech Republic*
[10]*Institute of Physics, Academy of Sciences, Center for Particle Physics, Prague, Czech Republic*
[11]*Universidad San Francisco de Quito, Quito, Ecuador*
[12]*Laboratoire de Physique Corpusculaire, IN2P3-CNRS, Université Blaise Pascal, Clermont-Ferrand, France*
[13]*Laboratoire de Physique Subatomique et de Cosmologie, IN2P3-CNRS, Universite de Grenoble 1, Grenoble, France*
[14]*CPPM, IN2P3-CNRS, Université de la Méditerranée, Marseille, France*
[15]*Laboratoire de l'Accélérateur Linéaire, IN2P3-CNRS, Orsay, France*
[16]*LPNHE, Universités Paris VI and VII, IN2P3-CNRS, Paris, France*
[17]*DAPNIA/Service de Physique des Particules, CEA, Saclay, France*
[18]*IReS, IN2P3-CNRS, Université Louis Pasteur, Strasbourg, France and Université de Haute Alsace, Mulhouse, France*
[19]*Institut de Physique Nucléaire de Lyon, IN2P3-CNRS, Université Claude Bernard, Villeurbanne, France*
[20]*RWTH Aachen, III. Physikalisches Institut A, Aachen, Germany*
[21]*Universität Bonn, Physikalisches Institut, Bonn, Germany*
[22]*Universität Freiburg, Physikalisches Institut, Freiburg, Germany*
[23]*Universität Mainz, Institut für Physik, Mainz, Germany*
[24]*Ludwig-Maximilians-Universität München, München, Germany*
[25]*Fachbereich Physik, University of Wuppertal, Wuppertal, Germany*
[26]*Punjab University, Chandigarh, India*
[27]*Tata Institute of Fundamental Research, Mumbai, India*
[28]*University College Dublin, Dublin, Ireland*
[29]*Korea Detector Laboratory, Korea University, Seoul, Korea*
[30]*CINVESTAV, Mexico City, Mexico*
[31]*FOM-Institute NIKHEF and University of Amsterdam/NIKHEF, Amsterdam, The Netherlands*
[32]*University of Nijmegen/NIKHEF, Nijmegen, The Netherlands*
[33]*Joint Institute for Nuclear Research, Dubna, Russia*
[34]*Institute for Theoretical and Experimental Physics, Moscow, Russia*

[35]*Moscow State University, Moscow, Russia*
[36]*Institute for High Energy Physics, Protvino, Russia*
[37]*Petersburg Nuclear Physics Institute, St. Petersburg, Russia*
[38]*Lund University, Lund, Sweden; Royal Institute of Technology and Stockholm University, Stockholm, Sweden; and Uppsala University, Uppsala, Sweden*
[39]*Lancaster University, Lancaster, United Kingdom*
[40]*Imperial College, London, United Kingdom*
[41]*University of Manchester, Manchester, United Kingdom*
[42]*University of Arizona, Tucson, Arizona 85721, USA*
[43]*Lawrence Berkeley National Laboratory and University of California, Berkeley, California 94720, USA*
[44]*California State University, Fresno, California 93740, USA*
[45]*University of California, Riverside, California 92521, USA*
[46]*Florida State University, Tallahassee, Florida 32306, USA*
[47]*Fermi National Accelerator Laboratory, Batavia, Illinois 60510, USA*
[48]*University of Illinois at Chicago, Chicago, Illinois 60607, USA*
[49]*Northern Illinois University, DeKalb, Illinois 60115, USA*
[50]*Northwestern University, Evanston, Illinois 60208, USA*
[51]*Indiana University, Bloomington, Indiana 47405, USA*
[52]*University of Notre Dame, Notre Dame, Indiana 46556, USA*
[53]*Iowa State University, Ames, Iowa 50011, USA*
[54]*University of Kansas, Lawrence, Kansas 66045, USA*
[55]*Kansas State University, Manhattan, Kansas 66506, USA*
[56]*Louisiana Tech University, Ruston, Louisiana 71272, USA*
[57]*University of Maryland, College Park, Maryland 20742, USA*
[58]*Boston University, Boston, Massachusetts 02215, USA*
[59]*Northeastern University, Boston, Massachusetts 02115, USA*
[60]*University of Michigan, Ann Arbor, Michigan 48109, USA*
[61]*Michigan State University, East Lansing, Michigan 48824, USA*
[62]*University of Mississippi, University, Mississippi 38677, USA*
[63]*University of Nebraska, Lincoln, Nebraska 68588, USA*
[64]*Princeton University, Princeton, New Jersey 08544, USA*
[65]*Columbia University, New York, New York 10027, USA*
[66]*University of Rochester, Rochester, New York 14627, USA*
[67]*State University of New York, Stony Brook, New York 11794, USA*
[68]*Brookhaven National Laboratory, Upton, New York 11973, USA*
[69]*Langston University, Langston, Oklahoma 73050, USA*
[70]*University of Oklahoma, Norman, Oklahoma 73019, USA*
[71]*Brown University, Providence, Rhode Island 02912, USA*
[72]*University of Texas, Arlington, Texas 76019, USA*
[73]*Southern Methodist University, Dallas, Texas 75275, USA*
[74]*Rice University, Houston, Texas 77005, USA*
[75]*University of Virginia, Charlottesville, Virginia 22901, USA*
[76]*University of Washington, Seattle, Washington 98195, USA*

(Received 20 October 2004; published 11 May 2005)

The ratio of the $B^+$ and $B^0$ meson lifetimes was measured using data collected in 2002–2004 by the D0 experiment in Run II of the Fermilab Tevatron Collider. These mesons were reconstructed in $B \to \mu^+ \nu D^{*-} X$ decays, which are dominated by $B^0$ and $B \to \mu^+ \nu \bar{D}^0 X$ decays, which are dominated by $B^+$. The ratio of lifetimes is measured to be $\tau^+/\tau^0 = 1.080 \pm 0.016(\text{stat}) \pm 0.014(\text{syst})$.

DOI: 10.1103/PhysRevLett.94.182001 PACS numbers: 14.40.Nd

In the last few years, significant progress has been made in the understanding of the lifetimes of hadrons containing heavy quarks. Charm and bottom meson (except $B_c$) lifetimes have been measured with precisions ranging from 0.5 to 4%, although lifetimes of heavy baryons are not known as well [1]. Experimentally, ratios of lifetimes have smaller uncertainties, since many common sources of systematics cancel. Theoretical uncertainties for these ratios are also reduced. For instance, the ratio of the $B^+$ and $B^0$ lifetimes has been predicted to be $1.06 \pm 0.02$ [2,3].

In this Letter, we present a measurement of the ratio of $B^+$ and $B^0$ lifetimes using semileptonic decays $B \to \mu^+ \nu \bar{D}^0 X$ [4] collected by the D0 experiment at Fermilab in $p\bar{p}$ collisions at $\sqrt{s} = 1.96$ TeV. The data correspond to approximately 440 $\text{pb}^{-1}$ of integrated luminosity.

The D0 detector is described in detail elsewhere [5]. The primary vertex of the $p\bar{p}$ interaction was determined for each event with the precision on average about 20 $\mu$m in the plane perpendicular to the beam pipe and about 40 $\mu$m along the beam pipe. Events with semimuonic $b$-hadron decays were selected using a suite of inclusive single-muon triggers in a three-level trigger system. Muons were required to have a transverse momentum $p_T^\mu > 2$ GeV/$c$ and total momentum $p^\mu > 3$ GeV/$c$. $\bar{D}^0$ candidates were selected using $\bar{D}^0 \to K^+\pi^-$ decays. All charged particles in an event were clustered into jets using the DURHAM algorithm [6] with a jet $p_T$ cutoff parameter of 15 GeV/$c$ [7]. A $\bar{D}^0$ candidate was constructed from two particles of opposite charge belonging to the same jet as the muon. Both particles were required to have $p_T > 0.7$ GeV/$c$ and to form a common $\bar{D}^0$ vertex. The $p_T$ of the $\bar{D}^0$ was required to exceed 5 GeV/$c$. To reduce the combinatorial background, we required the $\bar{D}^0$ vertex to have a positive displacement in the plane perpendicular to the beam pipe, relative to the primary vertex, with at least $4\sigma$ significance. The trajectory of the muon and $\bar{D}^0$ candidates were required to originate from a common $B$ vertex. The $\mu^+\bar{D}^0$ system was required to have an invariant mass between 2.3 and 5.2 GeV/$c^2$.

The masses of the kaon and pion were assigned to the two tracks according to the charge of the muon, assuming the $\mu^+K^+\pi^-$ combination. The mass spectrum of the $K\pi$ system after these selections is shown in Fig. 1(a). The signal in the $\bar{D}^0$ peak contains 126 073 $\pm$ 610 events.

The reconstructed $\mu^+\bar{D}^0$ events were classified into three nonoverlapping samples, based on the presence of an additional pion with $p_T > 0.18$ GeV/$c$. Defining $\Delta m = m(\bar{D}^0\pi) - m(\bar{D}^0)$, all events containing a pion with a charge opposite to (same as) that of the muon and $0.1425 < \Delta m < 0.1490$ GeV/$c^2$ were included in the $D^{*-R}(D^{*-W})$ sample. The $D^{*-W}$ sample contains true $\bar{D}^0$ but fake $D^{*-}$ events and gives an estimate of the combinatorial background for $\mu^+D^{*-}$ candidates. All other events were assigned to the $\bar{D}^0$ sample. Figure 1(b) shows the $\Delta m$ distributions, when $1.8 < m(\bar{D}^0) < 1.9$ GeV/$c^2$.

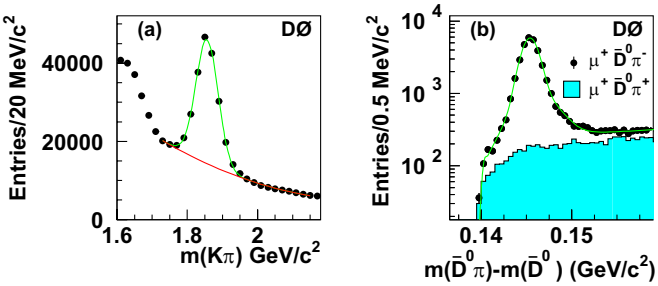


FIG. 1 (color online). (a) Invariant mass of the $K\pi$ system. The curve shows the result of the fit of the $K^+\pi^-$ mass distribution with the sum of a signal Gaussian function and polynomial background function. (b) Mass difference $\Delta m = m(\bar{D}^0\pi) - m(\bar{D}^0)$.

The peak in the sample with opposite charges of muon and pion corresponds to the production of the $\mu^+D^{*-}$ system and contains 30 528 $\pm$ 200 events.

The classification into these samples was based on the presence of a slow pion from $D^{*-} \to \bar{D}^0\pi^-$ decay, and was independent of the $B$-meson lifetime. Therefore, the ratio of the number of events in the two samples, expressed as a function of the proper decay length, depends mainly on the lifetime difference between the $B^+$ and $B^0$ mesons. The influences of the selection criteria, detector properties, and some systematic uncertainties are significantly reduced.

Since the final state has missing particles, including the neutrino, the proper decay length was not determined. Instead, the measured visible proper decay length $x^M$ was computed as $x^M = m_B c(\boldsymbol{L}_T \cdot \boldsymbol{p}_T(\mu^+\bar{D}^0))/|\boldsymbol{p}_T(\mu^+\bar{D}^0)|^2$. $\boldsymbol{L}_T$ is the vector from the primary to the $\mu\bar{D}^0$ vertex in the plane perpendicular to the beam pipe, $\boldsymbol{p}_T(\mu^+\bar{D}^0)$ is the transverse momentum of the $\mu^+\bar{D}^0$ system and $m_B = 5.279$ GeV/$c^2$ is the mass of the $B$ meson [1]. To reduce the difference between the $D^{*-}$ and $\bar{D}^0$ samples, the pion from the $D^{*-}$ decay was not used for the computation of the transverse momentum and the decay length.

Candidates in each of the samples were divided into eight groups according to their $x^M$ values. The number of $\mu^+\bar{D}^0$ events $N_i^{*R}$ (from the $D^{*-R}$ sample), $N_i^{*W}$ (from the $D^{*-W}$ sample), and $N_i^0$ (from the $\bar{D}^0$ sample) in each interval $i$ ($i = 1, \ldots, 8$) were determined from the fit of the $K\pi$ mass spectrum between 1.72 and 2.16 GeV/$c^2$ with the sum of a Gaussian signal function and a polynomial background function. The mean and width of the Gaussian function were fixed to the values obtained from the fit of the overall mass distribution in each sample. The fitting procedure was the same for all samples.

The number of $\mu^+D^{*-}$ events for each interval $i$ of $x^M$ was defined as $N_i(\mu^+D^{*-}) = N_i^{*R} - CN_i^{*W}$, where $CN_i^{*W}$ accounts for the combinatorial background under the $D^{*-}$ peak as shown in Fig. 1(b). The coefficient $C = 1.27 \pm 0.03$ reflects the difference in the combinatorial background between $\mu^+\bar{D}^0\pi^-$ and $\mu^+\bar{D}^0\pi^+$ events. It was determined from the ratio of the numbers of these events in the interval $0.153 < \Delta m < 0.160$ GeV/$c^2$. The number of $\mu^+\bar{D}^0$ events in each interval $i$ in $x^M$ was defined as $N_i(\mu^+\bar{D}^0) = N_i^0 + N_i^{*W} + CN_i^{*W}$.

The experimental observable $r_i$ is the ratio of $\mu^+D^{*-}$ and $\mu^+\bar{D}^0$ events in interval $i$ of $x^M$, i.e., $r_i = N_i(\mu^+D^{*-})/N_i(\mu^+\bar{D}^0)$. Values of $r_i$ and statistical uncertainties are given in Table I. The value of $k \equiv \tau^+/\tau^0 - 1$ was determined from the minimization of $\chi^2(\varepsilon_\pi, k)$ which has the following form:

$$\chi^2(\varepsilon_\pi, k) = \sum_i \frac{[r_i - r_i^e(\varepsilon_\pi, k)]^2}{\sigma^2(r_i)}. \quad (1)$$

Here $r_i^e(\varepsilon_\pi, k)$ is the expected ratio of $\mu^+D^{*-}$ and $\mu^+\bar{D}^0$ events, and $\varepsilon_\pi$ is the efficiency to reconstruct the slow pion in the $D^{*-} \to \bar{D}^0\pi^-$ decay. $\varepsilon_\pi$ was assumed to be inde-

TABLE I. Definition of the intervals in visible proper decay length, $x^M$. For each interval $i$, the ratio $r_i$, and the expected value $r_i^e$ for $\tau^+/\tau^0 - 1 = 0.080$ are given.

| $i$ | $x^M$ range (cm) | $r_i$ | $r_i^e$ |
|---|---|---|---|
| 1 | −0.1–0.0 | 0.295 ± 0.015 | 0.309 |
| 2 | 0.0–0.02 | 0.321 ± 0.007 | 0.315 |
| 3 | 0.02–0.04 | 0.317 ± 0.007 | 0.313 |
| 4 | 0.04–0.07 | 0.305 ± 0.006 | 0.308 |
| 5 | 0.07–0.10 | 0.295 ± 0.007 | 0.300 |
| 6 | 0.10–0.15 | 0.282 ± 0.007 | 0.291 |
| 7 | 0.15–0.25 | 0.283 ± 0.009 | 0.276 |
| 8 | 0.25–0.40 | 0.274 ± 0.019 | 0.256 |

pendent of $x^M$ and, along with $k$, was a free parameter in the minimization. The sum $\sum_i$ was taken over all intervals with positive $x^M$.

For the $j$th $B$ meson decay channel, the distribution of the visible proper decay length ($x$) is given by $P_j(x) = \int dK D_j(K)\theta(x)\frac{K}{c\tau_j}\exp(-\frac{Kx}{c\tau_j})$. $\tau_j$ is the lifetime of the $B$ meson, the $K$ factor, $K = p_T^{\mu^+\bar{D}^0}/p_T^B$, reflects the difference between the observed and true momentum of the $B$ meson, and $\theta(x)$ is the step function. The function $D_j(K)$ is the normalized distribution of the $K$ factor for the $j$th decay channel.

Transformation from the true value of $x$ to the experimentally measured value $x^M$ is given by $f_j(x^M) = \int dx R_j(x - x^M)\varepsilon_j(x)P_j(x)$, where $R_j(x - x^M)$ is the detector resolution, and $\varepsilon_j(x)$ is the reconstruction efficiency of $\mu^+\bar{D}^0$ for the $j$th decay. It does not include $\varepsilon_\pi$ for channels with $D^{*-}$. Finally, the expected value $r_i^e(\varepsilon_\pi, k)$ is given by

$$r_i^e(\varepsilon_\pi, k) = \frac{\varepsilon_\pi F_i^*(k)}{F_i^0(k) + (1 - \varepsilon_\pi)F_i^*(k)}. \quad (2)$$

Here $F_i^{*,0} = \int_i dx^M \sum_j \mathrm{Br}_j f_j(x^M)$ with the summation $\sum_j$ taken over all decays to $D^{*-}(\bar{D}^0)$ for $F_i^*(F_i^0)$.

For the computation of $r_i^e$, the world average of the $B^+$ lifetime [1] was used. The $B^0$ lifetime $\tau^0$ was expressed as $\tau^0 = \tau^+/(1 + k)$. The branching fractions $B \to \mu^+\nu\bar{D}$ and $B \to \mu^+\nu\bar{D}^*$ were taken from Ref. [1]. The following branching fractions were derived from experimental measurements [1,8–10]: $\mathrm{Br}(B^+ \to \mu^+\nu\bar{D}^{**0}) = (2.67 \pm 0.37)\%$, $\mathrm{Br}(B^+ \to \mu^+\nu\bar{D}^{**0} \to D^{*-}X) = (1.07 \pm 0.25)\%$, and $\mathrm{Br}(B_s^0 \to \mu^+\nu D_s^{**-}) = (2.3^{+2.4}_{-2.3})\%$. $D^{**}$ states include both narrow and wide $D^{**}$ resonances and nonresonant $DX$ and $D^*X$ production. Regarding the possible decays of $D_s^{**-}$, there is no experimental data on the $\mathrm{Br}(D_s^{**-} \to D^{*-}X)$. Its central value was therefore set to 0.35, and it was varied between 0.0 and 1.0 to estimate the systematic uncertainty from this source. All other branching fractions were derived assuming isospin invariance.

The distributions $D_j(K)$, $R_j(x)$, and $\varepsilon_j(x)$ were taken from the Monte Carlo simulation. All processes involving $b$ hadrons were simulated using the EVTGEN [11] generator interfaced to PYTHIA [7] and followed by the full modeling of the detector response and event reconstruction. The semileptonic $b$ hadron decays were generated using the ISGW2 model [12].

Assuming the given branching fractions and reconstruction efficiencies, the decay $B \to \mu^+ D^{*-}X$ contains $(89 \pm 3)\%B^0$, $(10 \pm 3)\%B^+$, and $(1 \pm 1)\%B_s^0$, while the decay $B \to \mu^+\bar{D}^0X$ contains $(83 \pm 3)\%B^+$, $(15 \pm 4)\%B^0$, and $(2 \pm 1)\%B_s^0$.

Our study showed that the decay $B \to \tau^+\bar{D}^0X \to \mu^+\nu\bar{\nu}\bar{D}^0X$ adds $(5 \pm 2)\%$, and the process $c\bar{c} \to \mu^+\bar{D}^0X$ adds $(10 \pm 7)\%$ to the selected $\mu^+\bar{D}^0$ sample. The latter estimate also includes a possible contribution from $c\bar{c} \to h^+\bar{D}^0X$, when hadron $h^+$ is misidentified as muon. These processes were taken into account in the analysis. The $B \to \bar{D}^0D_sX$ decay was found to be strongly suppressed by the applied kinematic cuts, contributing less than 2.0%, and was neglected.

Using all these inputs, the minimization of the $\chi^2$ distribution, Eq. (1), gives $k \equiv \tau^+/\tau^0 - 1 = 0.080 \pm 0.016(\mathrm{stat})$. The $\chi^2$ at the minimum is 4.2 for 5 d.o.f., $\varepsilon_\pi$ is $0.864 \pm 0.006(\mathrm{stat})$, and the global correlation coefficient between $k$ and $\varepsilon_\pi$ is 0.18. The simulation predicted $\varepsilon_\pi = 0.877 \pm 0.003$. The reasonable agreement in $\varepsilon_\pi$ between data and simulation reflects good consistency of input efficiencies and branching fractions with experimental data. Figure 2 presents the $r_i$ values together with the result of the fit.

The influence of various sources of systematic uncertainty on the final result is summarized in Table II. Different contributions can be divided into three groups. The first part includes uncertainties coming from the experimental measurements, e.g., branching fractions and lifetimes. All inputs were varied by 1 standard deviation. Only the most significant contributions are listed as indi-

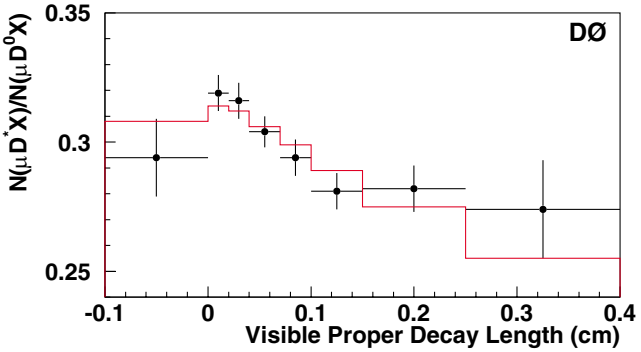


FIG. 2 (color online). Points with the error bars show the ratio of the number of events in the $\mu^+D^{*-}$ and $\mu^+\bar{D}^0$ samples as a function of the visible proper decay length. The result of the minimization of Eq. (1) with $k = 0.080$ is shown as a histogram.

TABLE II. Summary of systematic uncertainties.

| Source | $\Delta(\tau^+/\tau^0)$ |
|---|---|
| $\mathrm{Br}(B^0 \to \mu^+ \nu D^{*-})$ | 0.0005 |
| $\mathrm{Br}(B^+ \to \mu^+ \nu \bar{D}^{*0})$ | 0.0010 |
| $\mathrm{Br}(B^+ \to \mu^+ \nu \bar{D}^{**0})$ | 0.0009 |
| $\mathrm{Br}(B^+ \to \mu^+ \nu D^{*-} \pi^+ X)$ | 0.0059 |
| $\mathrm{Br}(B_s^0 \to \mu^+ \nu D_s^- X)$ | 0.0009 |
| $D_s^{**-} \to D^{*-} X$ | 0.0020 |
| $c\bar{c} \to \mu^+ \nu \bar{D}^0 X$ contribution | 0.0015 |
| Other contributions | 0.0006 |
| $\varepsilon(B \to \mu^+ \nu \bar{D}^0 X)$, decay length dependence | 0.0014 |
| Modeling $B$ meson decays | 0.0030 |
| $\varepsilon_\pi$, decay length dependence | 0.0036 |
| Decay length resolution | 0.0024 |
| Difference in $D^{*-}$ and $\bar{D}^0$ resolution | 0.0053 |
| $K$ factors, average value | 0.0032 |
| $K$ factors, difference between channels | 0.0013 |
| Fitting procedure | 0.0086 |
| Background level under $D^{*-}$ | 0.0004 |
| Total | 0.0136 |

vidual entries in Table II; all remaining uncertainties are combined into a single entry ''Other contributions.''

The second group includes uncertainties due to the inputs taken from the Monte Carlo simulation. The uncertainty due to the decay length dependence of the efficiencies $\varepsilon(B \to \mu^+ \nu \bar{D}^0 X)$ was obtained by repeating the analysis with decay length independent efficiencies used for all decay modes.

The variation of the efficiency from channel to channel arises from differences in the kinematics of $B$-meson decays and thus depends on their modeling in simulation. To estimate the uncertainty from this source, an alternative model [13] of semileptonic $B$ decays with parameters $\rho^2 = 0.92$, $R_1 = 1.18$, and $R_2 = 0.72$ was used. In addition, the selection cuts on the $p_T$ of the $\mu^+$ and $\bar{D}^0$ were varied over a wide range.

The same alternative model and the variation of $p_T$ cuts were used to study the model dependence of the $K$ factors. In all cases, the variation of the average value of $K$ factors did not exceed 2%. Distributions of $K$ factors were determined separately for $B \to \mu^+ \nu \bar{D}^0$, $B \to \mu^+ \nu \bar{D}^*$, $B \to \mu^+ \nu \bar{D}^{**} \to \bar{D}^0 X$, and $B \to \mu^+ \nu \bar{D}^{**} \to \bar{D}^* X$. To estimate the uncertainty due to the modeling of $\bar{D}^{**}$ decays, which include both resonant and nonresonant components and are not yet well understood, the analysis was repeated with the distributions of $K$ factors from $B \to \bar{D}^{**} \to \bar{D}^0(\bar{D}^*)$ decays set to be the same as for $B \to \bar{D}^0(\bar{D}^*)$ decays.

The selection of the slow pion was made independently of the $B$ lifetime, and the efficiency $\varepsilon_\pi$ was assumed constant in the minimization. A dedicated study of $K_S^0 \to \pi^+ \pi^-$ decays showed good stability of the track reconstruction efficiency with the change of decay length over a wide range. The slope in the efficiency was estimated to be $0.0038 \pm 0.0059\ \mathrm{cm}^{-1}$. The independence of $\varepsilon_\pi$ and the decay length was also verified in simulation. The impact on the systematic uncertainty in $k$ of the possible lifetime dependence of $\varepsilon_\pi$ was estimated by repeating the analysis with $\varepsilon_\pi$ varying within the simulation statistical error.

The average decay length resolution, approximately 35 $\mu$m for this measurement, and the fraction of events with larger resolution, modeled by a Gaussian function with resolution of 1700 $\mu$m, were varied over a wide range, significantly exceeding the estimated difference in resolution between data and simulation. The corresponding change of $k$ was taken as the systematic uncertainty from this source.

The number of events with negative decay length is determined by the resolution; therefore, the difference between the expected and the observed ratios $r_1$ of events with negative decay length (the first row in Table I) could indicate the difference in resolution between $D^*$ and $D^0$ samples. Supposing that the whole deviation of $r_1$ from the expected value is caused by such a difference, and by varying the resolution of $D^0$ sample, while keeping the resolution of $D^*$ sample to be the same, it is possible to obtain an exact agreement of observed and expected values of $r_1$. The fit was repeated with this modified resolution and the change of $k$ was used as the estimate of systematic uncertainty due to the difference in resolution between $D^*$ and $D^0$ samples.

The fitting procedure is another source of systematic uncertainty. To estimate it, different parametrizations of background functions and variation of the fit limits were used. For the signal description, the fit with two Gaussians and the fit with the mean and width allowed to vary were tried. Kaons and pions cannot be separated by the D0 detector, and the decays $\bar{D}^0 \to K^+ K^-$ and $\bar{D}^0 \to \pi^+ \pi^-$ are also present in the $K^+ \pi^-$ mass spectrum. The fit was repeated with the signal taken as the sum of the Gaussian for the $\bar{D}^0 \to K^+ \pi^-$ decay and template $m(K^+ \pi^-)$ distributions for the $\bar{D}^0 \to K^+ K^-$ and $\bar{D}^0 \to \pi^+ \pi^-$ decays, when the particles were assigned the masses of $K^+ \pi^-$. These template distributions were taken from simulation. The relative rate of different decay modes was taken from [1]. The maximal variation of the result obtained was taken as the systematic uncertainty due to this source. Finally, the uncertainty in the background level under the $D^{*-}$ peak in Fig. 1(b) was also taken into account.

Various consistency checks of this measurement were also performed. The total sample of events was divided into two parts using different criteria, such as the sign of the muon rapidity, polarity of the solenoid, charge of the muon, $p_T$ of the muon, position of the primary interaction, etc. The measurement was repeated independently for each sample. The definition of proper decay length intervals was varied, one more interval, 0.4–0.8 cm, was added, and the last interval, 0.25–0.4 cm, was removed from the fit. In all

cases, the results are consistent within statistical uncertainties. Finally, the measurement of the ratio of lifetimes was performed with simulated events. The resulting value $k^{\mathrm{MC}} = 0.084 \pm 0.015$ agrees well with the generated lifetime ratio $k^{\mathrm{gen}} = 0.070$. The whole fitting procedure was also verified to the precision 0.0005 in $k$ using a fast simulation.

In summary, the ratio of $B^+$ and $B^0$ meson lifetimes was found to be

$$k = \frac{\tau^+}{\tau^0} - 1 = 0.080 \pm 0.016(\mathrm{stat}) \pm 0.014(\mathrm{syst}). \quad (3)$$

This result is the most precise measurement of this parameter, and agrees well with the world average value $k = 0.086 \pm 0.017$ [1]. Improved precision of the ratio of $B^+$ and $B^0$ lifetimes will allow a better test of theoretical predictions, especially those inputs to the calculations that rely on lattice QCD or on other nonperturbative methods [2,3].

We thank the staffs at Fermilab and collaborating institutions, and acknowledge support from the DOE and NSF (USA), CEA and CNRS/IN2P3 (France), FASI, Rosatom, and RFBR (Russia), CAPES, CNPq, FAPERJ, FAPESP, and FUNDUNESP (Brazil), DAE and DST (India), Colciencias (Colombia), CONACyT (Mexico), KRF (Korea), CONICET and UBACyT (Argentina), FOM (The Netherlands), PPARC (United Kingdom), MSMT (Czech Republic), CRC Program, CFI, NSERC, and WestGrid Project (Canada), BMBF and DFG (Germany), SFI (Ireland), A.P. Sloan Foundation, Research Corporation, Texas Advanced Research Program, Alexander von Humboldt Foundation, and the Marie Curie Fellowships.

*Visitor from University of Zurich, Zurich, Switzerland.
†Visitor from Institute of Nuclear Physics, Krakow, Poland.

[1] S. Eidelman *et al.* (Particle Data Group), Phys. Lett. B **592**, 1 (2004).
[2] G. Bellini *et al.*, Phys. Rep. **289**, 1 (1997).
[3] E. Franco *et al.*, Nucl. Phys. **B633**, 212 (2002); M. Benke *et al.*, Nucl. Phys. **B639**, 389 (2002).
[4] Charge conjugate states are always implied in this Letter.
[5] V. Abazov *et al.* (D0 collaboration), Nucl. Instrum. Methods Phys. Res., Sect. A, "The Upgraded D0 Detector" (to be published).
[6] S. Catani *et al.*, Phys. Lett. B **269**, 432 (1991).
[7] T. Sjöstrand *et al.*, Comput. Phys. Commun. **135**, 238 (2001).
[8] D. Buskulic *et al.* (ALEPH Collaboration), Z. Phys. C **73**, 601 (1997).
[9] P. Abreu *et al.* (DELPHI Collaboration), Phys. Lett. B **475**, 407 (2000).
[10] D. Abbaneo *et al.*, hep-ex/0112028.
[11] D. J. Lange, Nucl. Instrum. Methods Phys. Res., Sect. A **462**, 152 (2001).
[12] D. Scora and N. Isgur, Phys. Rev. D **52**, 2783 (1995).
[13] M. Neubert, Phys. Rep. **245**, 259 (1994).